



## Self-Interacting Dark Matter Can Explain Diverse Galactic Rotation Curves

Ayuki Kamada,<sup>1,2</sup> Manoj Kaplinghat,<sup>3</sup> Andrew B. Pace,<sup>3,4</sup> and Hai-Bo Yu<sup>1</sup>

<sup>1</sup>*Department of Physics and Astronomy, University of California, Riverside, California 92521, USA*

<sup>2</sup>*Institute for Basic Science, Center for Theoretical Physics of the Universe, Daejeon 34051, South Korea*

<sup>3</sup>*Department of Physics and Astronomy, University of California, Irvine, California 92697, USA*

<sup>4</sup>*George P. and Cynthia Woods Mitchell Institute for Fundamental Physics and Astronomy, and Department of Physics and Astronomy, Texas A&M University, College Station, Texas 77843, USA*

(Received 23 November 2016; revised manuscript received 23 June 2017; published 13 September 2017)

The rotation curves of spiral galaxies exhibit a diversity that has been difficult to understand in the cold dark matter (CDM) paradigm. We show that the self-interacting dark matter (SIDM) model provides excellent fits to the rotation curves of a sample of galaxies with asymptotic velocities in the 25–300 km/s range that exemplify the full range of diversity. We assume only the halo concentration-mass relation predicted by the CDM model and a fixed value of the self-interaction cross section. In dark-matter-dominated galaxies, thermalization due to self-interactions creates large cores and reduces dark matter densities. In contrast, thermalization leads to denser and smaller cores in more luminous galaxies and naturally explains the flatness of rotation curves of the highly luminous galaxies at small radii. Our results demonstrate that the impact of the baryons on the SIDM halo profile and the scatter from the assembly history of halos as encoded in the concentration-mass relation can explain the diverse rotation curves of spiral galaxies.

DOI: [10.1103/PhysRevLett.119.111102](https://doi.org/10.1103/PhysRevLett.119.111102)

*Introduction.*—The  $\Lambda$ CDM model, with a cosmological constant ( $\Lambda$ ) and cold dark matter (CDM), explains the observed large-scale structure of the Universe [1] and many aspects of galaxy formation [2,3], but the diverse observed rotation curves do not have a satisfactory explanation. Observations of a number of dwarf and low surface brightness galaxies indicate that the inner halo is often badly fit by the cusped halos predicted by  $\Lambda$ CDM simulations [4–13]. The core densities exhibit almost an order of magnitude spread for similar total halo masses [14], and galaxies with densities at the upper end of the range are consistent with  $\Lambda$ CDM [15]. There is no clear explanation for the diversity in the inner rotation velocity profiles of different galaxies within similar mass halos [15]. Although uncertainties remain for individual galaxies due to systematic errors in deriving rotation curves and modeling non-equilibrium and noncircular motions (see, e.g., [16–19]), it remains to be seen if these can provide a comprehensive explanation for the diversity.

In this Letter, we demonstrate how this diversity problem [15] can be solved in the self-interacting dark matter (SIDM) framework [20,21], where dark matter (DM) particles exchange energy by colliding with one another in halos. DM self-interactions change only the inner halo properties in accord with observations, leaving all the successes of CDM intact on large scales (see, e.g., [22–25]). Constraints from galaxy clusters demand an interaction cross section that diminishes with increasing velocity [21,24,26–28], which can be naturally accommodated in concrete particle physics models [21,29–38] (see [39] for a review).

The diversity in the observed rotation curves is solved by a combination of interconnected features in the  $\Lambda$ SIDM model. In the outer parts of galaxies, the  $\Lambda$ SIDM model is the same as the  $\Lambda$ CDM model, inheriting all its successes. In the inner regions, the SIDM density profile and its relation to the baryons is changed by the process of thermalization due to the self-interactions. The physical effects of thermalization in the inner region are varied but fully determined by the distribution of the baryons, up to the scatter from the assembly history. The fact that the baryons have a large role in creating the diversity, which we explicitly demonstrate here, has also been argued previously [40]. In many galaxies, thermalization forces particles out of the center and leads to a lower circular velocity than the DM-only  $\Lambda$ CDM predictions. In other galaxies where stars dominate the gravitational potential, the SIDM halo profile can be as steep as the  $\Lambda$ CDM predictions. In these galaxies, the total rotation curve is forced to be flat even at radii much smaller than the scale radius of the DM halo, providing a natural explanation to the disk-halo conspiracy [41]. All of the features discussed above are captured in a simple model that we discuss next.

*Modeling the SIDM halo with a stellar disk.*—We have developed an analytical method to model the SIDM halo properties [21,42], which is based on the isothermal solutions to the Jeans equations. The method has been tested against cosmological SIDM-only simulations [21] and isolated simulations of a range of galaxy types including baryons [28].

We divide the halo into two regions, separated by a characteristic radius  $r_1$  where the average scattering rate per particle times the halo age is equal to unity. The value of  $r_1$

is determined by the condition  $\langle\sigma v\rangle\rho(r_1)t_{\text{age}}/m \approx 1$ , where  $\sigma$  is the scattering cross section,  $m$  is the DM particle mass,  $v$  is the DM relative velocity,  $t_{\text{age}}$  is the age of the galaxy, and  $\langle\dots\rangle$  denotes averaging over the velocity distribution. In this Letter, we assume  $\sigma/m = 3 \text{ cm}^2/\text{g}$  and  $t_{\text{age}} = 10 \text{ Gyr}$  for all the galaxies motivated by previous results [21].

For radii  $r < r_1$ , SIDM particles experience multiple collisions over the age of galaxies and reach kinetic equilibrium. The density profile is  $\rho_{\text{iso}}(\vec{r}) = \rho_0 \exp[-\Phi_{\text{tot}}(\vec{r})/\sigma_{v0}^2]$ , where  $\rho_0$  is the central DM density,  $\sigma_{v0}$  is the one-dimensional DM velocity dispersion, and  $\Phi_{\text{tot}}$  is the total gravitational potential due to dark and baryonic matter normalized such that  $\Phi_{\text{tot}}(0) = 0$ . We note that features in the stellar or gas potential get imprinted in  $\rho_{\text{iso}}$  through  $\Phi_{\text{tot}}$ ; while we do not model such baryonic features here, we expect they will be more *strongly* reflected in the rotation curve [43] in SIDM than CDM. Since DM self-interactions rapidly thermalize the inner halo in the presence of baryons, the final SIDM density profile for the large cross sections considered here should be close to its equilibrium prediction, which depends on how the baryons are distributed but not on the formation history.

Assuming that the baryons are distributed in a thin disk with central surface density  $\Sigma_0$  and scale radius  $R_d$ , we can write the Poisson equation for  $\Phi_{\text{tot}}$  as

$$\nabla^2\Phi_{\text{tot}}(R, z) = 4\pi G[\rho_{\text{iso}}(R, z) + \Sigma_0 e^{-R/R_d}\delta(z)], \quad (1)$$

where  $\delta(z)$  is the Dirac delta function. We solve Eq. (1) by expanding it in the Legendre polynomials and parametrize the solution by two dimensionless parameters defined as  $a \equiv 8\pi G\rho_0 R_d^2/(2\sigma_{v0}^2)$  and  $b \equiv 8\pi G\Sigma_0 R_d/(2\sigma_{v0}^2)$  [44]. We have calculated 300 templates in total with different combinations of  $a$  and  $b$  values and interpolated between them as required.

For  $r > r_1$ , where scattering has occurred less than once per particle on average, we model the DM density as the Navarro-Frenk-White (NFW) profile  $\rho_{\text{NFW}}(r) = \rho_s(r/r_s)^{-1}(1+r/r_s)^{-2}$  seen in  $\Lambda$ CDM simulations [45]. We create the SIDM profile by joining the spherically averaged isothermal ( $\rho_{\text{iso}}$ ) and the spherical NFW ( $\rho_{\text{NFW}}$ ) profiles at  $r = r_1$  such that the mass and density are continuous at  $r_1$ . For  $\sigma/m = \mathcal{O}(1) \text{ cm}^2/\text{g}$ , the matching implies that  $r_1$  is close to  $r_s$  [23]. The SIDM halo parameters ( $\rho_0, \sigma_{v0}$ ) directly map onto  $(r_s, \rho_s)$  or  $(M_{200}, c_{200})$  of the NFW profile for a fixed  $\sigma/m$ . We assume that the large-scale structure is the same as that in the Planck  $\Lambda$ CDM model [1] and impose its halo concentration-mass relation on our solutions,  $c_{200} = 10^{0.905 \pm 0.11} (M_{200}/10^{12} h^{-1} M_\odot)^{-0.101}$  [46], while allowing for the expected scatter 0.11 dex scatter ( $1\sigma$ ).

*Halo concentration and the role of baryons.*—In the top panel in Fig. 1, we show the circular velocity due to the DM halo,  $V_{\text{cir,DM}}(r)$ , as a function of the radius for the SIDM and the corresponding CDM halos for  $V_{\text{max}} = 70 \text{ km/s}$ . It is clear that DM self-interactions

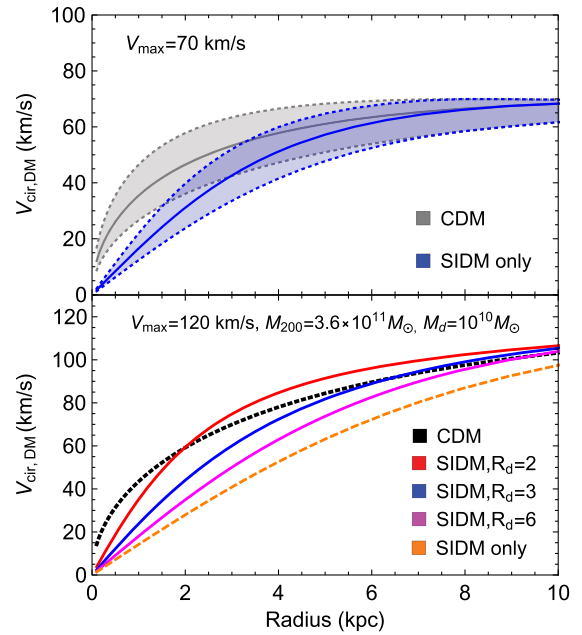


FIG. 1. Top: Circular velocity of the SIDM halo and the corresponding CDM halo for  $V_{\text{max}} = 70 \text{ km/s}$  with the  $2\sigma$  spread in halo concentration. Bottom: Circular velocity of the SIDM halo with  $V_{\text{max}} = 120 \text{ km/s}$  and median concentration including the impact of a stellar disk of mass  $M_d = 10^{10} M_\odot$  for three disk scale lengths  $R_d = 2, 3, \text{ and } 6 \text{ kpc}$ . The corresponding SIDM (dashed curves) and CDM (dotted curves) circular velocities without disks are also shown.

can lower circular velocity systematically in the inner regions. To assess the scatter quantitatively, we use  $V_{\text{cir}}(2 \text{ kpc})$  [15]. At large radii  $r \gtrsim r_1$ , both halos have the same  $V_{\text{cir,DM}}(r)$ , but the SIDM halos have significantly smaller  $V_{\text{cir,DM}}(2 \text{ kpc})$ . The  $2\sigma$  scatter in  $V_{\text{cir,DM}}(2 \text{ kpc})$  (from the scatter in the concentration-mass relation) is about a factor of 1.8 in SIDM similar to that in CDM (about 1.6).

Observationally,  $V_{\text{cir}}(2 \text{ kpc})$  (total rotation velocity) spans from 20 to 70 km/s for  $V_{\text{max}} \sim 70 \text{ km/s}$  [15]. The SIDM prediction for the lowest  $V_{\text{cir}}(2 \text{ kpc})$  is consistent with 20 km/s. When baryons are included, the upper end of the predicted range for  $V_{\text{cir}}(2 \text{ kpc})$  changes significantly. Beyond contributing directly to the total  $V_{\text{cir}}$ , its presence changes the total potential  $\Phi_{\text{tot}}$ , and the equilibrium isothermal solution is consequently denser [42]. The net effect is to increase the upper end of the predicted range for  $V_{\text{cir}}(2 \text{ kpc})$  to 70 km/s, fully consistent with the data.

For larger galaxies, even the low end of the predicted  $V_{\text{cir,DM}}(2 \text{ kpc})$  can be changed by the presence of the baryons. We illustrate this in the bottom panel in Fig. 1. We adopt  $V_{\text{max}} = 120 \text{ km/s}$  and median concentration for the halo. We set the total disk mass to be  $10^{10} M_\odot$  (typical for this halo mass) and vary the scale radius of the thin disk  $R_d = 2, 3, \text{ and } 6 \text{ kpc}$ . We use the matching

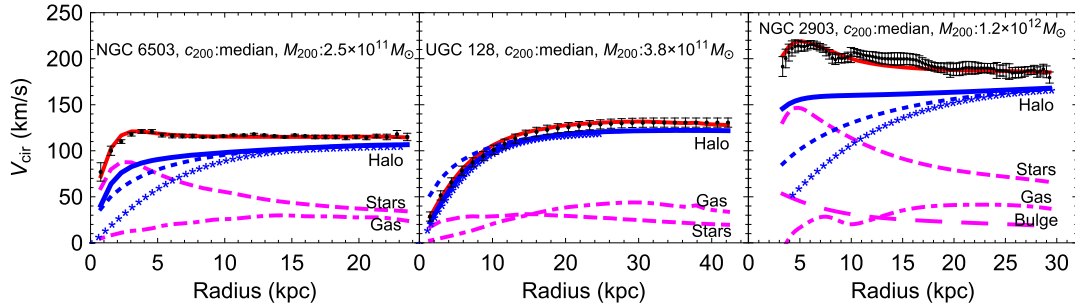


FIG. 2. The left two panels show the SIDM fits to the rotation curves of NGC 6503 and UGC 128. They asymptote to  $V_f \approx 130$  km/s in the outer parts, but their inner rotation curves are very different. The right panel shows the SIDM fit to a highly luminous galaxy, NGC 2903. The total fit is displayed in red, and it includes contributions from the SIDM halo (blue solid curve), stars (magenta dashed curve), gas (magenta dot-dashed curve), and bulge (magenta long-dashed curve). The predictions of the corresponding CDM halo (dotted curve) and the SIDM halo neglecting the influence of the baryons (asterisk curve) are also shown.

procedure described above to obtain the SIDM halo mass profiles. With  $R_d = 2$  kpc, the SIDM prediction for  $V_{\text{cir,DM}}(2 \text{ kpc})$  is very close to the CDM prediction. The scatter in  $V_{\text{cir,DM}}(2 \text{ kpc})$  from changing  $R_d$  is almost a factor of 2; even the disk with  $R_d = 6$  kpc has some effect on the SIDM halo. Thus, the SIDM inner halo mass profile is strongly correlated with the distribution of the baryons, which, along with the scatter from the concentration-mass relation, leads to the diversity in the SIDM halo properties. These facets of thermalization in SIDM have been confirmed by  $N$ -body simulations of galaxies [47].

*Solving the diversity problem in SIDM models.*—To explicitly demonstrate how the diversity is accommodated in SIDM, we fit to the rotation curves of 30 galaxies that maximize the diversity and have an asymptotic circular velocity  $V_f$  in the 25–300 km/s range. We obtained excellent fits overall, with  $\chi^2/\text{d.o.f.} < 1$  for 23 galaxies (DDO 52, 154, 87 126; UGC 128, 5005, 11707, 4483, 3371, 5721, 12506, 1281; UGCA 442; NGC 2366, 7331, 2403, 3109, 1560, 2903, 3198; F583-1, F579-V1, M33) and  $\chi^2/\text{d.o.f.} < 2$  for the rest (UGC 2841, 5750; NGC 6503, F571-8, F563-V2, DDO 133, IC 2574) using data from Refs. [8, 11, 48–62]. In Figs. 2 and 3, we show the fits to some of the most extreme examples highlighted in Ref. [15]. (In Supplemental Material [63], we show the fits for the 24 other galaxies.) For each galaxy, we compute the

thin disk parameters ( $\Sigma_0, R_d$ ) that best match the rotation curves of the stellar disk in the literature, given a value of the mass-to-light ratio ( $\Upsilon_*$ ). In computing  $\rho_{\text{iso}}$ , we have neglected the potential of the gaseous disk and stellar bulge, which is a good approximation for the fits shown here. In our fits, the outer halo  $V_{\text{max}}$  is essentially set by the measured  $V_f$ , and the freedom in the fits is primarily due to  $\Upsilon_*$  and the scatter allowed in the concentration of the outer halo.

NGC 6503 [59] and UGC 128 [53] clearly illustrate the diverse features in the rotation curves caused by the baryon distribution in Fig. 2. Both galaxies have  $V_f \approx 130$  km/s, but their inner rotation curves are very different. For NGC 6503, the circular velocity increases sharply in the inner regions and reaches its asymptotic value around 3 kpc; in UGC 128, it increases very mildly and reaches  $V_f$  at 20 kpc. Despite the dramatic differences, the SIDM halo with *median* concentration provides a remarkable fit to both galaxies. NGC 6503 is a high surface brightness galaxy, and its inner gravitational potential is dominated by the stellar disk, which contributes significantly to the observed  $V_{\text{cir}}$ . Moreover, the inner SIDM (isothermal) halo density in the presence of the disk is almost an order of magnitude larger than when neglecting the influence of the disk, which boosts the halo contribution at  $V_{\text{cir}}(2 \text{ kpc})$  from 20 to 60 km/s. In contrast, the stellar disk has a negligible effect

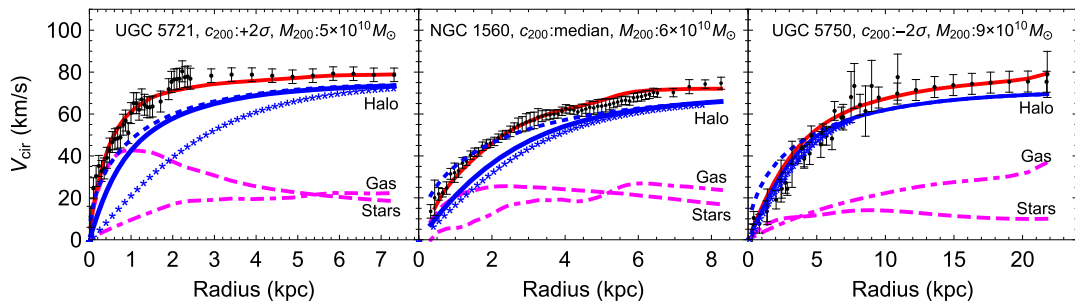


FIG. 3. SIDM fits (red solid curve) to the rotation curves of spiral galaxies UGC 5721, NGC 1560, and UGC 5750, all with  $V_f \approx 80$  km/s but showing extreme diversity in the inner parts. Line types are the same as in Fig. 2.



on the SIDM halo of UGC 128. With the effects of thermalization included properly, the rotation curves of both high and low surface brightness galaxies are consistent with the SIDM model, contrary to previous analytic expectations [64]. For comparison, we have plotted the NFW halo  $V_{\text{cir}}$  profiles with the same  $(M_{200}, c_{200})$  values as our SIDM fits in Figs. 2 and 3. (If the NFW profile is forced to fit a large sample of rotation curves, then the inferred  $c_{200}$  values have substantially larger scatter than  $\Lambda$ CDM predictions [65], which is also evident in our fits to the 30 galaxies.)

It is interesting to note that in NGC 6503 the rotation curve becomes flat at  $r \approx 3$  kpc, which implies that the total density profile scales as a power law in radius, with an index close to  $-2$ , from inner regions dominated by the disk to outer regions dominated by DM. Thus, the thermalization of DM provides a natural mechanism for understanding the long-standing puzzle of the disk-halo conspiracy [41]. This power-law behavior of the total mass density is prevalent in large spiral and elliptical galaxies [66,67]. We show the SIDM fit to the rotation curve of massive spiral galaxy NGC 2903 [11] in the right panel in Fig. 2 as an example.

In Fig. 3, we show SIDM fits for UGC 5721 [51,52], NGC 1560 [58], and UGC 5750 [8,53–55]. All have similar  $V_f \approx 80$  km/s, but the shapes of the rotation curves are very different in the inner regions. UGC 5721 and UGC 5750 are at opposite extremes for the rotation curve diversity in this mass range. Despite the diversity, the SIDM halo model provides an impressive fit to them. We find that NGC 1560 has a median halo, UGC 5721 has a denser halo, and UGC 5750 has an underdense halo, but all within  $2\sigma$  of the median expectation. The observed  $V_{\text{cir}}(2 \text{ kpc})$  is close to 20 km/s for UGC 5750, while the corresponding CDM halo has  $V_{\text{cir}}(2 \text{ kpc}) \approx 30$  km/s even with a concentration  $2\sigma$  lower than the median value. The effect of the disk is most significant in UGC 5721, resulting in a SIDM halo *similar* to the CDM one and a flat  $V_{\text{cir}}$  even at 2 kpc. The effect becomes mild in NGC 1560 and negligible in UGC 5750, consistent with their luminosities. We have checked that UGC 5721 can also be fit with a  $1.5\sigma$  higher  $c_{200}$  value and  $M_{200} = 6 \times 10^{10} M_{\odot}$ , and UGC 5720 with a  $1.5\sigma$  lower  $c_{200}$  and  $M_{200} = 8 \times 10^{10} M_{\odot}$ , due to a mild  $c_{200}$ - $M_{200}$  degeneracy.

*Diversity from uniformity.* The diversity problem is solved by a combination of features in  $\Lambda$ SIDM that are not separate pieces to be tuned but instead arise from the requirement that the inner halo at  $r \lesssim r_1$  is thermalized. While the inner rotation curves display great diversity for the same halo mass, there are also remarkable similarities. In Fig. 4, we plot a measure of the surface density of DM defined as  $\Sigma_{\text{DM},0} = \rho_0 r_c$ , where  $r_c$  is the core radius where the DM density is half of the central density  $\rho_0$ .

The minimal sample (squares) shows a clear scaling relation for  $\Sigma_{\text{DM},0}$  vs  $V_{\text{max}}$  (of the NFW halo), which is a reflection of the concentration-mass relation [68]. Our model

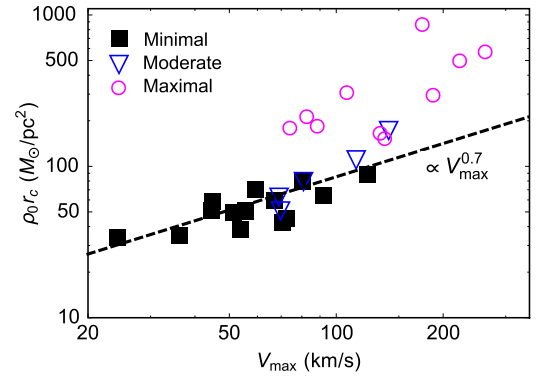


FIG. 4. The inferred SIDM core density times core radius (“surface density”) for the 30 galaxies we have fit. The “minimal” sample is composed of DM-dominated galaxies for which baryons do not change the SIDM profile significantly. The surface densities of these galaxies scale as  $V_{\text{max}}^{0.7}$  (dashed line), which can be traced to the concentration-mass relation. The “intermediate” sample shows progressively increasing effects of the stellar disk on the SIDM halo, while the “maximal” one has the most significant effects, where the baryons dominate the inner regions.

predicts  $\Sigma_{\text{DM},0} \propto V_{\text{max}}^{0.7}$ , which may be roughly understood from the approximate scalings  $r_c \propto r_s$  [23] and  $\rho_0 \propto V_{\text{max}}^2/r_s^2$  from dimensional arguments. However, there is a clear deviation when baryons become important (triangles and circles), since  $\rho_0$  increases and the core radius is set by the gravitational potential of the baryons. Our  $\Sigma_{\text{DM},0}$  values for the minimal sample are consistent with previous results [69].

*Self-interaction cross section.*—We fixed  $\sigma/m = 3 \text{ cm}^2/\text{g}$  in our analysis, and it provided good fits for all 30 galaxies with  $c_{200}$  values within the  $2\sigma$  range and mass-to-light ratios in the range preferred by recent measurements [70–72]. Galaxies with low  $V_{\text{cir}}(2 \text{ kpc})$  like UGC 5750 and IC 2574 drive the preference for this large  $\sigma/m$ . However, there are degeneracies among  $\sigma/m$ ,  $\Upsilon_*$  and  $c_{200}$ . For higher luminosity galaxies, in particular, those with  $V_f \gtrsim 200$  km/s such as NGC 2903, 7331, and 2841 and UGC 12560, good fits can also be found with smaller cross sections,  $\sigma/m \sim 1 \text{ cm}^2/\text{g}$ , by varying  $\Upsilon_*$  very mildly. This implies that a mild velocity dependence, which would be required by the galaxy cluster constraints [21,28,38], is also consistent with the data. We have checked that the  $\Upsilon_*$  values (disk masses) required by the fits are consistent with abundance matching expectations [73].

*Conclusions.*—The rotation curves of spiral galaxies exhibit considerable diversity, which lacks an explanation. The problem is most severe for galaxies with flat rotation velocities around 100 km/s. To address this problem in the context of SIDM models, we developed numerical templates for modeling the SIDM halo including the presence of a stellar disk and fit a wide variety of rotation curves for spiral galaxies that exemplify the diversity over 3 orders of magnitude in total mass. Our model utilizes the  $\Lambda$ CDM

concentration-mass relation and a fixed self-interaction cross section. We have demonstrated that the variation in the distribution of baryons and the reaction of the SIDM halo to it, when melded with the expected scatter in the concentration-mass relation due to the assembly history of halos, can explain the diverse DM distributions in spiral galaxies.

We thank Erwin de Blok, Gianfranco Gentile, Federico Lelli, Stacy McGaugh, Se-Heon Oh, and Rob Swaters for providing us the rotation curve data. This work was supported by Institute for Basic Science under the project code IBS-R018-D1 (A. K.), the National Science Foundation Grants No. PHY-1620638 (M. K.) and No. PHY-1522717 (A. B. P.), and the U.S. Department of Energy under Grant No. DE-SC0008541 (H.-B. Y.). A. B. P. acknowledges support from a GAANN fellowship and the Mitchell Institute for Fundamental Physics and Astronomy at Texas A&M University. H.-B. Y. acknowledges support from the Hellman Fellows Fund.

- 
- [1] P. A. R. Ade *et al.* (Planck Collaboration), *Astron. Astrophys.* **571**, A16 (2014).
- [2] V. Springel, C. S. Frenk, and S. D. M. White, *Nature (London)* **440**, 1137 (2006).
- [3] S. Trujillo-Gomez, A. Klypin, J. Primack, and A. J. Romanowsky, *Astrophys. J.* **742**, 16 (2011).
- [4] R. A. Flores and J. R. Primack, *Astrophys. J.* **427**, L1 (1994).
- [5] B. Moore, *Nature (London)* **370**, 629 (1994).
- [6] A. Burkert, *Astrophys. J.* **447**, L25 (1995); *IAU Symp.* **171**, 175 (1996).
- [7] M. Persic, P. Salucci, and F. Stel, *Mon. Not. R. Astron. Soc.* **281**, 27 (1996).
- [8] W. J. G. de Blok and A. Bosma, *Astron. Astrophys.* **385**, 816 (2002).
- [9] G. Gentile, P. Salucci, U. Klein, D. Vergani, and P. Kalberla, *Mon. Not. R. Astron. Soc.* **351**, 903 (2004).
- [10] R. Kuzio de Naray, S. S. McGaugh, and W. de Blok, *Astrophys. J.* **676**, 920 (2008).
- [11] W. J. G. de Blok, F. Walter, E. Brinks, C. Trachternach, S.-H. Oh, and R. C. Kennicutt, Jr., *Astron. J.* **136**, 2648 (2008).
- [12] S.-H. Oh, W. de Blok, E. Brinks, F. Walter, and Robert C. J. Kennicutt, *Astron. J.* **141**, 193 (2011).
- [13] S.-H. Oh *et al.*, *Astron. J.* **149**, 180 (2015).
- [14] R. K. de Naray, G. D. Martinez, J. S. Bullock, and M. Kaplinghat, *Astrophys. J.* **710**, L161 (2010).
- [15] K. A. Oman *et al.*, *Mon. Not. R. Astron. Soc.* **452**, 3650 (2015).
- [16] K. A. Oman, J. F. Navarro, L. V. Sales, A. Fattahi, C. S. Frenk, T. Sawala, M. Schaller, and S. D. M. White, *Mon. Not. R. Astron. Soc.* **460**, 3610 (2016).
- [17] J. I. Read, G. Iorio, O. Agertz, and F. Fraternali, *Mon. Not. R. Astron. Soc.* **462**, 3628 (2016).
- [18] J. C. B. Pineda, C. C. Hayward, V. Springel, and C. Mendes de Oliveira, *Mon. Not. R. Astron. Soc.* **466**, 63 (2017).
- [19] K. El-Badry, A. Wetzel, M. Geha, P. F. Hopkins, D. Kereš, T. K. Chan, and C.-A. Faucher-Giguère, *Astrophys. J.* **820**, 131 (2016).
- [20] D. N. Spergel and P. J. Steinhardt, *Phys. Rev. Lett.* **84**, 3760 (2000).
- [21] M. Kaplinghat, S. Tulin, and H.-B. Yu, *Phys. Rev. Lett.* **116**, 041302 (2016).
- [22] M. Vogelsberger, J. Zavala, and A. Loeb, *Mon. Not. R. Astron. Soc.* **423**, 3740 (2012).
- [23] M. Rocha, A. H. G. Peter, J. S. Bullock, M. Kaplinghat, S. Garrison-Kimmel, J. Oñorbe, and L. A. Moustakas, *Mon. Not. R. Astron. Soc.* **430**, 81 (2013).
- [24] A. H. Peter, M. Rocha, J. S. Bullock, and M. Kaplinghat, *Mon. Not. R. Astron. Soc.* **430**, 105 (2013).
- [25] M. Vogelsberger, J. Zavala, F.-Y. Cyr-Racine, C. Pfrommer, T. Bringmann, and K. Sigurdson, *Mon. Not. R. Astron. Soc.* **460**, 1399 (2016).
- [26] C. Firmani, E. D’Onghia, V. Avila-Reese, G. Chincarini, and X. Hernández, *Mon. Not. R. Astron. Soc.* **315**, L29 (2000).
- [27] N. Yoshida, V. Springel, S. D. M. White, and G. Tormen, *Astrophys. J.* **544**, L87 (2000).
- [28] O. D. Elbert, J. S. Bullock, M. Kaplinghat, S. Garrison-Kimmel, A. S. Graus, and M. Rocha, [arXiv:1609.08626](https://arxiv.org/abs/1609.08626).
- [29] J. L. Feng, M. Kaplinghat, and H.-B. Yu, *Phys. Rev. Lett.* **104**, 151301 (2010).
- [30] M. R. Buckley and P. J. Fox, *Phys. Rev. D* **81**, 083522 (2010).
- [31] A. Loeb and N. Weiner, *Phys. Rev. Lett.* **106**, 171302 (2011).
- [32] S. Tulin, H.-B. Yu, and K. M. Zurek, *Phys. Rev. Lett.* **110**, 111301 (2013).
- [33] S. Tulin, H.-B. Yu, and K. M. Zurek, *Phys. Rev. D* **87**, 115007 (2013).
- [34] J. M. Cline, Z. Liu, G. D. Moore, and W. Xue, *Phys. Rev. D* **90**, 015023 (2014).
- [35] K. K. Boddy, J. L. Feng, M. Kaplinghat, and T. M. P. Tait, *Phys. Rev. D* **89**, 115017 (2014).
- [36] K. Schutz and T. R. Slatyer, *J. Cosmol. Astropart. Phys.* **01** (2015) 021.
- [37] J. M. Cline, Z. Liu, G. D. Moore, and W. Xue, *Phys. Rev. D* **89**, 043514 (2014).
- [38] K. K. Boddy, M. Kaplinghat, A. Kwa, and A. H. G. Peter, *Phys. Rev. D* **94**, 123017 (2016).
- [39] S. Tulin and H.-B. Yu, [arXiv:1705.02358](https://arxiv.org/abs/1705.02358).
- [40] C. Brook, *Mon. Not. R. Astron. Soc.* **454**, 1719 (2015).
- [41] T. S. van Albada and R. Sancisi, *Phil. Trans. R. Soc. A* **320**, 447 (1986).
- [42] M. Kaplinghat, R. E. Keeley, T. Linden, and H.-B. Yu, *Phys. Rev. Lett.* **113**, 021302 (2014).
- [43] R. Sancisi, in *Dark Matter in Galaxies*, edited by S. Ryder, D. Pisano, M. Walker, and K. Freeman (Astronomical Society of the Pacific, San Francisco, 2004), IAU Symposium Vol. 220, p. 233.
- [44] N. Amorisco and G. Bertin, *Astron. Astrophys.* **519**, A47 (2010).
- [45] J. F. Navarro, C. S. Frenk, and S. D. White, *Astrophys. J.* **490**, 493 (1997).
- [46] A. A. Dutton and A. V. Macciò, *Mon. Not. R. Astron. Soc.* **441**, 3359 (2014).

- [47] P. Creasey, O. Sameie, L. V. Sales, H.-B. Yu, M. Vogelsberger, and J. Zavala, *Mon. Not. R. Astron. Soc.* **468**, 2283 (2017).
- [48] F. Lelli, M. Verheijen, F. Fraternali, and R. Sancisi, *Astron. Astrophys.* **544**, A145 (2012).
- [49] S.-H. Oh *et al.*, *Astron. J.* **149**, 180 (2015).
- [50] F. Lelli, S. S. McGaugh, and J. M. Schombert, *Astron. J.* **152**, 157 (2016).
- [51] R. A. Swaters, R. Sancisi, T. S. van Albada, and J. M. van der Hulst, *Astron. Astrophys.* **493**, 871 (2009).
- [52] R. A. Swaters, B. F. Madore, F. C. van den Bosch, and M. Balcells, *Astrophys. J.* **583**, 732 (2003).
- [53] J. M. van der Hulst, E. D. Skillman, T. R. Smith, G. D. Bothun, S. S. McGaugh, and W. J. G. de Blok, *Astron. J.* **106**, 548 (1993).
- [54] S. S. McGaugh, V. C. Rubin, and W. J. G. de Blok, *Astron. J.* **122**, 2381 (2001).
- [55] R. Kuzio de Naray, S. S. McGaugh, W. J. G. de Blok, and A. Bosma, *Astrophys. J. Suppl. Ser.* **165**, 461 (2006).
- [56] W. J. G. de Blok, S. S. McGaugh, and J. M. van der Hulst, *Mon. Not. R. Astron. Soc.* **283**, 18 (1996).
- [57] S.-H. Oh, W. J. G. de Blok, E. Brinks, F. Walter, and R. C. Kennicutt, Jr., *Astron. J.* **141**, 193 (2011).
- [58] G. Gentile, M. Baes, B. Famaey, and K. van Acoleyen, *Mon. Not. R. Astron. Soc.* **406**, 2493 (2010).
- [59] K. G. Begeman, Ph.D. thesis, Kapteyn Institute, 1987.
- [60] G. Gentile, G. I. G. Józsa, P. Serra, G. H. Heald, W. J. G. de Blok, F. Fraternali, M. T. Patterson, R. A. M. Walterbos, and T. Oosterloo, *Astron. Astrophys.* **554**, A125 (2013).
- [61] E. Corbelli, D. Thilker, S. Zibetti, C. Giovanardi, and P. Salucci, *Astron. Astrophys.* **572**, A23 (2014).
- [62] Z. S. Kam, C. Carignan, L. Chemin, P. Amram, and B. Epinat, *Mon. Not. R. Astron. Soc.* **449**, 4048 (2015).
- [63] See Supplemental Material at <http://link.aps.org/supplemental/10.1103/PhysRevLett.119.111102> for SIDM fits to the rotation curves of 30 spiral galaxies with asymptotic velocities in the 25–300 km/s range that exemplify the full range of diversity.
- [64] F. J. Sánchez-Salcedo, *Astrophys. J.* **631**, 244 (2005).
- [65] H. Katz, F. Lelli, S. S. McGaugh, A. Di Cintio, C. B. Brook, and J. M. Schombert, *Mon. Not. R. Astron. Soc.* **466**, 1648 (2017).
- [66] P. J. Humphrey and D. A. Buote, *Mon. Not. R. Astron. Soc.* **403**, 2143 (2010).
- [67] M. Cappellari *et al.*, *Astrophys. J.* **804**, L21 (2015).
- [68] H. W. Lin and A. Loeb, *J. Cosmol. Astropart. Phys.* **03** (2016) 009.
- [69] F. Donato, G. Gentile, P. Salucci, C. Frigerio Martins, M. I. Wilkinson, G. Gilmore, E. K. Grebel, A. Koch, and R. Wyse, *Mon. Not. R. Astron. Soc.* **397**, 1169 (2009).
- [70] T. P. K. Martinsson, M. A. W. Verheijen, K. B. Westfall, M. A. Bershadsky, D. R. Andersen, and R. A. Swaters, *Astron. Astrophys.* **557**, A131 (2013).
- [71] S. E. Meidt *et al.*, *Astrophys. J.* **788**, 144 (2014).
- [72] S. S. McGaugh and J. M. Schombert, *Astron. J.* **148**, 77 (2014).
- [73] S. Garrison-Kimmel, M. Boylan-Kolchin, J. Bullock, and K. Lee, *Mon. Not. R. Astron. Soc.* **438**, 2578 (2014).